Science Advances
AAAS

Supplementary Materials for

Skin and heart allograft rejection solely by long-lived alloreactive T_{RM} cells in skin of severe combined immunodeficient mice

Qianchuan Tian, Zhaoqi Zhang, Liang Tan, Fan Yang, Yanan Xu, Yinan Guo, Dong Wei, Changhong Wu, Peng Cao, Jiawei Ji, Wei Wang*, Xubiao Xie*, Yong Zhao*

*Corresponding author. Email: zhaoy@ioz.ac.cn (Y.Z.); xiexubiao@csu.edu.cn (X.X.); zico73@medmail.com.cn (W.W.)

Published 26 January 2022, *Sci. Adv.* **8**, eabk0270 (2022)
DOI: 10.1126/sciadv.abk0270

The PDF file includes:

Other Supplementary Material for this manuscript includes the following:

Supplementary Materials

Materials and Methods

Isolation of immune cells in skin and heart tissues

Skin and heart were quickly cut into small pieces with a scalpel, then digested for 60 min (for skin) or 40 min (for heart) at 37°C with 400 U/ml collagenase IV (Sigma-Aldrich), 10 mM HEPES and 0.01% DNase I (MP Biomedicals) in HBSS. Digested suspensions were passed through a nylon mesh. Then cells were collected after centrifugation at 300 3 g for 10 min. For cell surface marker staining, skin single cells were re-suspended in FACS staining buffer. For cytokine staining, cells were pre-incubated at 37ºC and 5% CO2 in RPMI + 10% FCS + 10 ng/mL PMA + 100 ng/mL ionomycin in the presence of GolgiPlug (BD) during 6 h. For intracellular staining, Fixation/Permeabilization Solution Kit (BD, cat# 554714) was used.

Flow cytometry

The cells from the harvested skin, hearts, and spleens were washed once with FACS buffer (PBS, pH 7.2, containing 0.1% NaN_3 and 0.5% bovine serum albumin). Then, cells were re-suspended in FACS buffer and stained with antibodies. The following anti-mouse mAbs used for cell staining were purchased from BD Biosciences Pharmingen (San Diego, CA, USA): anti-mCD69-PE, anti-mCD4-PE-Cy5, anti-mCD8-BV421, anti-mKi67-PE, anti-mCD44-FITC, anti-mCD62L-PE, anti-mIL-17A-PE, and anti-mIL-17F-APC. The following anti-mouse mAbs were purchased from eBioscience (San Diego, CA, USA): Fixable Viability Dye eFluor™ 506, anti-mCD103-FITC, anti-mCD45-APC, and anti-mF4/80-FITC. The following anti-mouse mAbs were purchased from Biolegend: anti-mTCRβ-PE-Cy7 and anti-mH-2D^d-PE. All flow cytometry data were obtained with an LSRFortessa™ X-20 instrument (BD Biosciences, CA, USA) and analyzed with FlowJo V 10 software (Treestar, OR, USA).

Adoptive transfer of $CD4^+$ T cells or $CD8^+$ T cells

Splenocytes from BALB/c mice were stained with CD4-PE, CD8-PE-Cy5, and TCRβ-APC-Cy7. The $CD4^+$ or $CD8^+$ T cells were sorted by MoFlo XDP sorter (Beckman), and 1×10^6 sorted BALB/c $CD4^+$ or $CD8^+$ T cells were adoptively transferred to MHC-matched immunodeficient SCID mice via the tail vein injection.

Quantitative PCR analysis

Total RNA was isolated with TRIzol (Invitrogen, Carlsbad, CA) and reverse transcribed with Superscript II (Qiagen) according to the manufacturer's instructions. The cDNA served as template for amplifying target genes and the housekeeping gene (HPRT) by real-time PCR. Target gene expression was calculated using the comparative method for relative quantification upon normalization to HPRT gene expression. Primers used in the present study are listed in Table 1.

Table 1. Primers used for qRT–PCR analysis.

Genes		Primer sequence (5'–3')
HPRT	Forward primer:	AGTACAGCCCCAAAATGGTTAAG
	Reverse primer:	CTTAGGCTTTGTATTTGGCTTTTC
Rorc	Forward primer:	GACCCACACCTCACAAATTGA
	Reverse primer:	AGTAGGCCACATTACACTGCT
IL-17A	Forward primer:	CTCAGACTACCTCAACCGTTCC
	Reverse primer:	ATGTGGTGGTCCAGCTTTCC
IL-17F	Forward primer:	CATACCCAGGAAGACATACTTAGAAG
	Reverse primer:	AGTCCCAACATCAACAGTAGC
IL-22	Forward primer:	CTGAGAAATGCTTGCGTCTG
	Reverse primer:	CGTTAGCTTCTCACTTTCCTTTAG
IL-23	Forward primer:	CTGAGAAGCAGGGAACAAGATG
	Reverse primer:	GAAGATGTCAGAGTCAAGCAGGTG
Tnfsf4	Forward primer:	TGCTTCATCTATGTCTGCCTG
	Reverse primer:	CTCACATCTGGTAACTGCTCC

Tnfsf8	Forward primer:	AGGAAATTGCTCAGAGGATCTC
	Reverse primer:	CTGGTATATGAGTCCGTGGATG
Lta	Forward primer:	CGCACAGCAGGTTCTCCACAT
	Reverse primer:	CCAACAAGGTGAGCAGCAGGTT
CCL1	Forward primer:	AGAGGCTTGAGACAGAAACTTATC
	Reverse primer:	GCAGCTATTGGAGACCGTAAG
CCL20	Forward primer:	TGGGTTTCACAAGACAGATGG
	Reverse primer:	GACTCTTAGGCTGAGGAGGTTC
CXCL1	Forward primer:	GCACCCAAACCGAAGTCATAG
	Reverse primer:	AGAAGCCAGCGTTCACCAGA
CXCL2	Forward primer:	GCCCAGACAGAAGTCATAGCC
	Reverse primer:	CTCCTCCTTTCCAGGTCAGTTA
CXCL9	Forward primer:	CCACTACAAATCCCTCAAAGAC
	Reverse primer:	TCTAGGCAGGTTTGATCTCC

RNA-seq analysis

We sorted naïve $CD4^+$T cells ($CD4^+CD62L^+CD44^{low}$) and $CD8^+$T cells ($CD8^+CD62L^+CD44^{low}$) from C57BL/6 mice by using an MoFlo XDP cell sorter (BeckMan Coulter, Brea, CA, USA). Total RNA was extracted using TRIzol agent (Thermo Fisher Scientific, 15596018). First strand cDNA synthesis and cDNA amplification was performed using Smart-Seq2 method. And Agilent 2100 High Sensitivity DNA Assay Kit (Agilent Technologies, CA, USA) was used to amplify the quality of products. Using Bioruptor Sonication System and CWBIO Gel Extraction Kit following manufacturer instructions, we performed library construction, then assessed and quantified the insertion size (library valid concentration >10 nM). The libraries were sequenced by an Illumina Hiseq platform with 150 bp paired end. The $CD4^+$ T_{RM} and $CD8^+$ T_{RM} cells were sorted by $CD4^+CD69^+$ and $CD8^+CD69^+$ cells in the skin from BALB/c mice at 100 days after the first allogeneic transplantation. The T_{RM} during the secondary allograft rejection were sorted by $CD4^+$ $CD69^+$ cells during the skin transplant rejection. All samples were collected in tubes containing lysis

components and ribonuclease inhibitors. All RNA extraction, library preparation, and sequencing were performed by Annoroad Gene Tech. (Beijing) Co., Ltd. The amplification was carried out by the Smart-Seq2 method. The qualified libraries were also loaded onto the Illumina HiSeq platform for the PE150 sequencing.

The mapping software HISAT2 was used to map the reads to the mouse mm10 reference genome and StringTie to construct transcripts independently for each cell (*32*). DEGseq was used to identify the differentially expressed genes. We set $q < 0.01$ and $|\log2(\text{foldchange})| > 1$ to a significant difference in the sensitive T_{RM} vs. T_{RM} during rejection comparison thresholds and set $q < 0.05$ and $|\log2(\text{foldchange})| > 0$ to a significant difference in the naïve T vs. sensitive T_{RM} comparison thresholds. Gene ontology (GO) functional annotation analysis was performed on all cell differential genes using the DAVID Bioinformatics Resources 6.8 online search tool (https://david.ncifcrf.gov/)(*58*). KEGG pathway analysis was performed on all the different genes of each cell using the KOBAS online search tool (http://kobas.cbi.pku.edu.cn/)(*59, 60*). The protein interaction network was obtained by STRING (https://string-db.org/) and visualized by Cytoscape (*61*).

Supplementary Figures

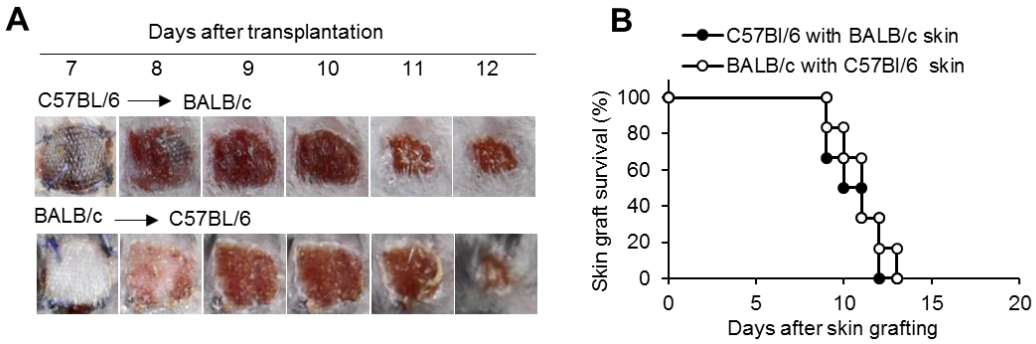

Fig. S1. Allogeneic skin graft rejection in immunocompetent recipient mice.

Rejection kinetics of C57BL/6 tail skin transplanted to BALB/c and BALB/c tail skin transplanted on C57BL/6. (A) Pictures for skin grafts at different days after grafting. (B) Allogeneic skin graft survival in BALB/c or C57BL/6 mice. n=5 per group.

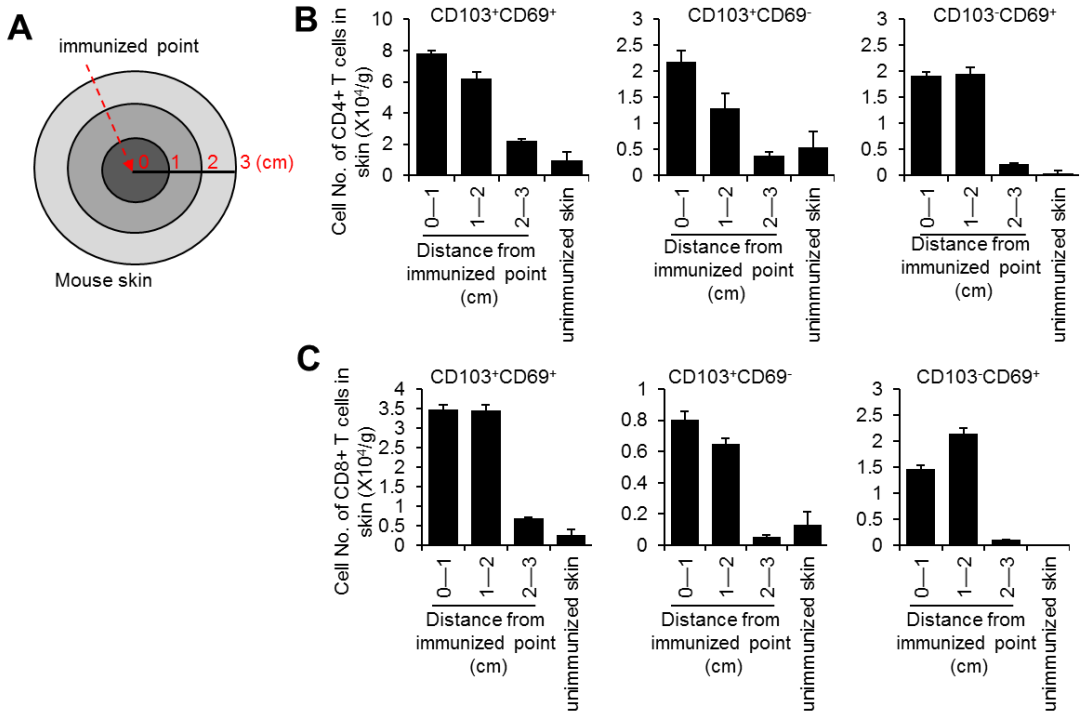

Fig. S2. The levels of T_{RM} cells in recipient skin tissues in different distance from the immunized site

(A) An abridged general view to show how to harvest the skin tissues at different distances from the immunized site in C57BL/6 skin-immunized BALB/c mice. Samples were harvested >60 days after skin grafting. (B) The cell number of $CD103^+CD69^+CD4^+$T cells, $CD103^+CD69^-CD4^+$T cells and $CD103^-CD69^+CD4^+$T cells in skin tissues at different distances (0–1 cm, 1–2cm, and 2–3cm) from the immunized point. (C) The number of $CD103^+CD69^+CD8^+$T cells, $CD103^+CD69^-CD8^+$T cells and $CD103^-CD69^+CD8^+$T cells in skin tissues at different distances (0–1 cm, 1–2cm, and 2–3cm) from the immunized point. Data were as means ± SD (n=5 per group). *$P < 0.05$, **$P < 0.01$, compared with the unimmunized mice.

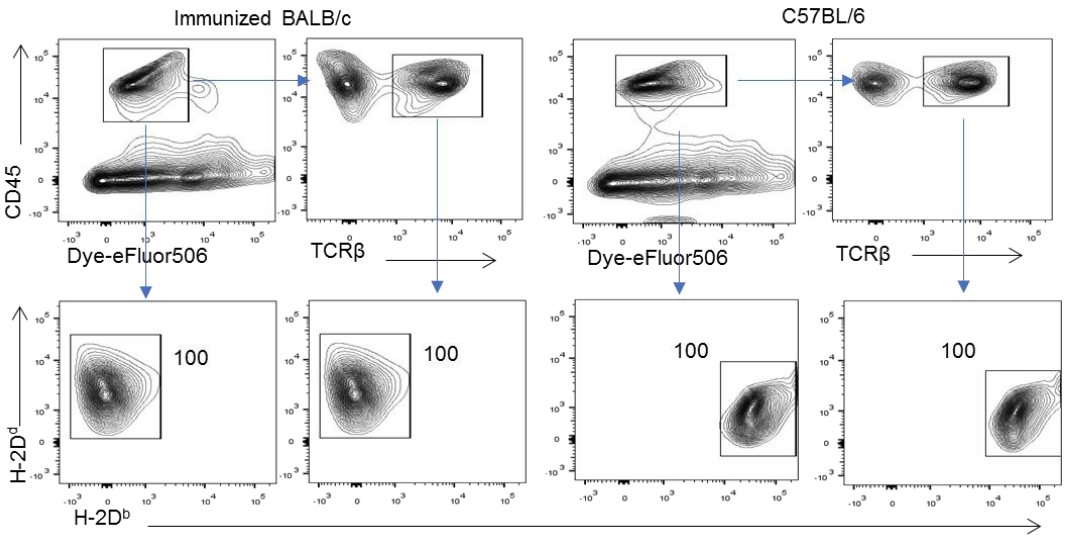

Fig. S3. The absence of donor-derived H-2D^{b+} immune and T cells in immunized BALB/c skin

Flow cytometric analysis of H-2D^{b} and H-2D^{d} in CD45^{+} and TCRβ^{+} cells in C57BL/6 skin-immunized BALB/c mice. C57BL/6 mouse skin was used as a positive control for H-2D^{b} Ab staining.

A TPM of genes in naïve CD8$^+$ T cells and induced CD8$^+$ T_{RM}

NAME	CD8$^+$ naïve T	Induced CD8$^+$ T_{RM}	q-value
Itgae	212.6266	398.6	7.52E-14
Cd69	749.554749	1543.247192	5.71E-62
Nr4a1	17.60304	287.8665	2.31E-61
Nr4a2	2.941558	469.1043	1.26E-104
Ctla4	4.854103	80.08604	3.92E-18
Cdh1	3.031012	72.17342	1.86E-17
Cd244	0.811938	8.125371	0.0052982
Prdm1	1.437966	5.91217	0.0399369
Rgs1	158.4129	4191.923	0
Rgs2	40.41766	2520.587	0
Fabp5	9.949105	161.196	6.98E-35
Bhlhe40	3.165554	308.5725	3.15E-43
S1pr1	592.748	50.93488	1.69E-114
Ccr7	1734.583	238.7452	1.72E-275
Sell	2043.933	19.69108	0
Hnf1a	0.778143	0	0.99

B TPM of genes in naïve CD4$^+$ T cells and Induced CD4$^+$ T_{RM}

NAME	CD4$^+$ naïve T	Induced CD4$^+$ T_{RM}	q-value
Itgae	7.871458	86.38226	9.51E-18
Cd69	1011.228	2879.709	3.86E-204
Nr4a1	85.39578	307.1277	3.34E-30
Nr4a2	3.812084	362.3801	7.64E-85
Ctla4	55.2963	579.6899	2.09E-108
Cdh1	0.64784	23.5601	3.96E-07
Cd244	1.563139	0.03277	0.0590746
Prdm1	8.371254	31.55357	8.69E-05
Rgs1	354.114	4910.296	0
Rgs2	87.66627	1912.042	0
Fabp5	7.860053	514.8943	7.69E-122
Bhlhe40	10.06881	193.6891	3.91E-72
S1pr1	693.2351	61.72812	2.04E-132
Ccr7	1729.056	337.5967	2.50E-222
Sell	1542.406	31.47326	0
Hnf1a	0.274315	0	9.90E-01

Fig. S4. Expression levels of some marker genes in the induced T_{RM}.

MARS (MA-plot-based method with Random Sampling model) method was used to identify differentially expressed genes in CD8$^+$ T_{RM} or CD4$^+$ T_{RM} cells. (A) The TPM of genes in naïve CD8$^+$ T cells and the induced CD8$^+$ T_{RM}. (B) The TPM of genes in naïve CD4$^+$ T cells and induced CD4$^+$ T_{RM}. The q-value of each gene compared between naïve T cells and the induced T_{RM} are shown in the table. The data are shown as heatmap figures in Figure 1C.

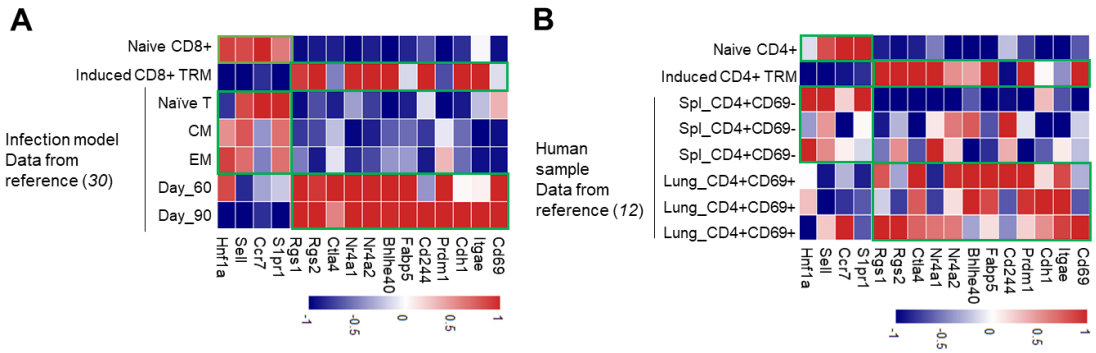

Fig. S5. The differential expressed genes in induced T_{RM}, naïve T cells, T_{CM}, and T_{EM} cells.

(A) The differential expressed genes in induced $CD8^+$ T_{RM}, naïve $CD8^+$ T cells, $CD8^+$ T_{CM}, $CD8^+$ T_{EM} cells, and $CD8^+$ T_{RM} at different days after infection. Some data were cited from reference (*30*). (B) The differential expressed genes in induced $CD4^+$ T_{RM}, naïve $CD4^+$ T cells, human splenic $CD4^+CD69^-$ T cells, and human lung $CD4^+CD69^+$ T_{RM}. Some data were cited from reference(*12*).

A Up-regulated pathways in $CD4^+$ T_{RM} during rejection compared with induced $CD4^+$ T_{RM}

Pathway	Pvalue
Ubiquitin mediated proteolysis	9.63E-08
Protein processing in endoplasmic reticulum	1.00E-07
Apoptosis	9.36E-07
TNF signaling pathway	9.89E-07
NF-kappa B signaling pathway	2.37E-06
Th17 cell differentiation	4.02E-06
Endocytosis	7.70E-06
Platelet activation	1.29E-05
Autophagy - animal	2.07E-05
Inositol phosphate metabolism	2.91E-05
Phosphatidylinositol signaling system	3.55E-05
Lysosome	0.000124
Regulation of actin cytoskeleton	0.000196
Cytokine-cytokine receptor interaction	0.000197
Natural killer cell mediated cytotoxicity	0.00023

B The expression of Th-related genes which were up-regulated and down-regulated in $CD4^+$ T_{RM} during graft rejection

Gene	Change	TRM	TRM during rejection	qvalue
Rorc	up	3.466398	17.48575	0.000784
Smad4	up	45.25118	131.9815	5.40E-11
Hif1a	up	249.2381	840.6531	4.20E-74
Ccr6	up	77.93236	175.2119	9.40E-10
Il18rap	up	8.584725	58.27309	2.61E-10
Il17a	up	0	1743.096	1.81E-213
Il17f	up	30.28435	2109.64	0
Il22	up	122.6038	1848.742	0
Tgfbr3	up	32.59842	58.90336	0.0027288
Runx3	up	55.45087	58.17526	0.2078105
Tnf	up	313.9238	374.5043	0.0087271
Cxcr3	up	43.16075	70.92978	0.0041335
Smad3	down	18.50295	7.549831	0.0118483
Tgfbr2	down	80.98253	67.03509	0.079067
Tbx21	down	106.3326	5.182178	2.67E-24
Gata3	down	277.631	86.40135	5.87E-24
Rxra	down	11.08842	1.690623	0.0027431
Ccl4	down	192.4087	1.756501	8.90E-45
Ccl5	down	1080.743	0	4.07E-149
Il12rb2	down	22.16243	5.918955	0.0008706
Pdlim5	down	76.69997	38.19008	0.0001845

Fig. S6. The shift of Th cell subsets-related genes in $CD4^+$ T_{RM} cells during graft rejection.

(A) The up-regulated pathways in the induced $CD4^+$ T_{RM} cells during graft rejection vs. the induced $CD4^+$ T_{RM} without rejection. (B) The altered expression of Th-related genes in activated $CD4^+$ T_{RM} during graft rejection compared with the induced $CD4^+$ T_{RM} without rejection.

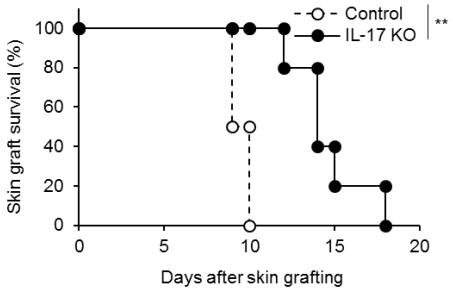

Fig. S7. BALB/c allogeneic skin graft rejection in Rag2KO mice with a piece of syngeneic immunized WT or IL-17KO skin tissue.

Thirty or more days after C57BL/6 or IL-17KO mice were immunized by BALB/c tail skin, one piece of the immunized C57BL/6 or IL-17KO mouse skin (2×2 cm) was harvested and grafted onto syngeneic Rag2KO mice. After Rag2KO mice were recovered for 30 days or so, a BALB/c tail skin was transplanted inside that 2×2 cm^2 immunized skin in Rag2KO mice. BALB/c skin graft survival in Rag2KO recipients with the immunized C57BL/6 or IL-17KO mouse skin tissue were shown (n=5 per group). **$P < 0.01$ compared between the indicated groups.